



Figures and figure supplements

Sleep-active neuron specification and sleep induction require FLP-11 neuropeptides to systemically induce sleep

Michal Turek *et al*

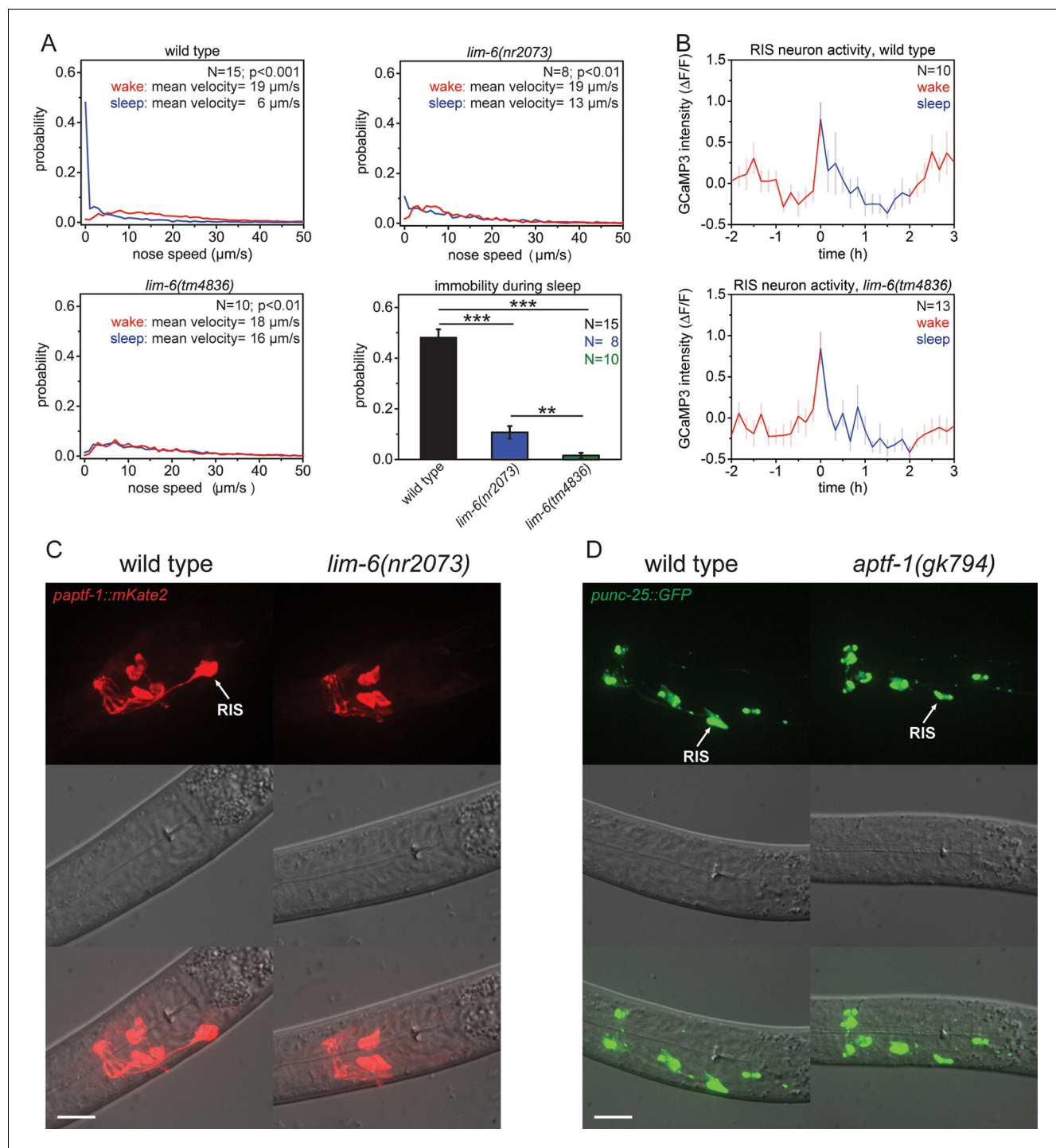


Figure 1. The LIM homeobox transcription factor LIM-6 controls sleep by specifying expression of the transcription factor APTF-1 in RIS. (A) Probability distribution of nose speeds during wake and sleep for wild type and *lim-6* mutants. *lim-6(nr2073)* shows substantially reduced and *lim-6(tm4836)* shows a complete lack of immobility during the time the animals should be sleeping. (B) Averaged RIS calcium activity pattern across time in wild type and *lim-6(tm4836)*. RIS is active at the onset of sleep in wild type and in *lim-6(tm4836)*. There was no statistically significant difference between wild-type and *lim-6* worms ($p > 0.05$, Welch test). (C) Expression of *paptf-1::mKate2* in wild type and *lim-6(nr2073)* L1 larvae. Expression of mKate2 is absent in RIS in *lim-6(nr2073)* showing that LIM-6 controls expression of APTF-1 in RIS. (D) Expression of *punc-25::GFP* in wild type and *aptf-1(gk794)*. Reporter GFP expression is normal in RIS in *aptf-1* mutant worms indicating that GABAergic function is not controlled by APTF-1. Statistical tests used were Wilcoxon Signed Paired Ranks test for comparison within the same genotype and Student's t-test for comparisons between genotypes. Error bars are SEM. ** denotes statistical significance with $p<0.01$, *** denotes statistical significance with $p<0.001$. Scale bars are 10 μm .

Figure 1 continued on next page

Figure 1 continued

DOI: [10.7554/eLife.12499.003](https://doi.org/10.7554/eLife.12499.003)

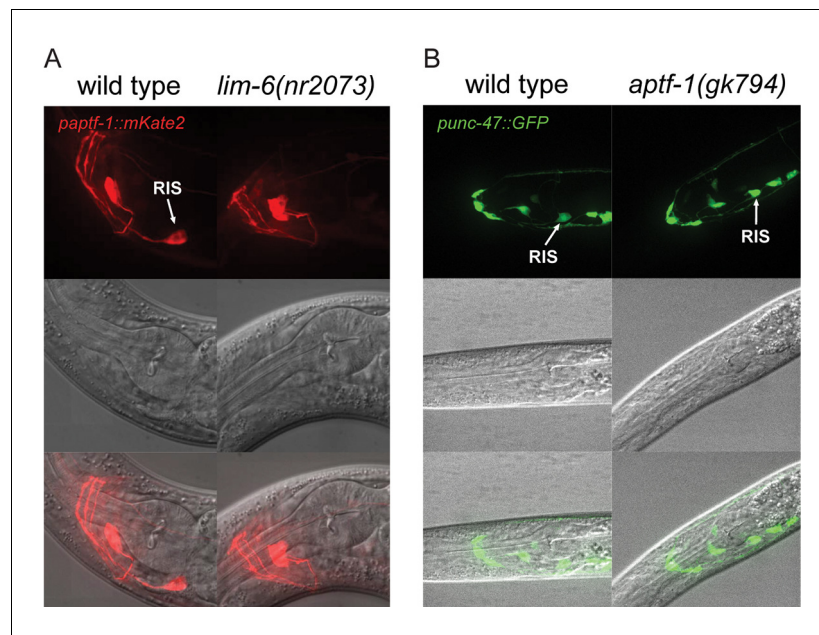


Figure 1—figure supplement 1. LIM-6 controls expression of APTF-1 across development but does not control the expression of the GABA vesicular transporter gene *unc-47*. **(A)** Expression of *paptf-1::mKate2* in wild type and in *lim-6(nr2073)* L4 larvae. Expression of *mKate2* is absent in RIS in *lim-6(nr2073)* at the L4 stage showing that LIM-6 generally controls expression of APTF-1 in RIS rather than the onset of expression. Scale bar is 10 μm. **(B)** *punc-47::GFP* is expressed in *aptf-1(gk794)* mutant worms. Shown are L1 larvae. Scale bar is 10 μm.

DOI: [10.7554/eLife.12499.004](https://doi.org/10.7554/eLife.12499.004)

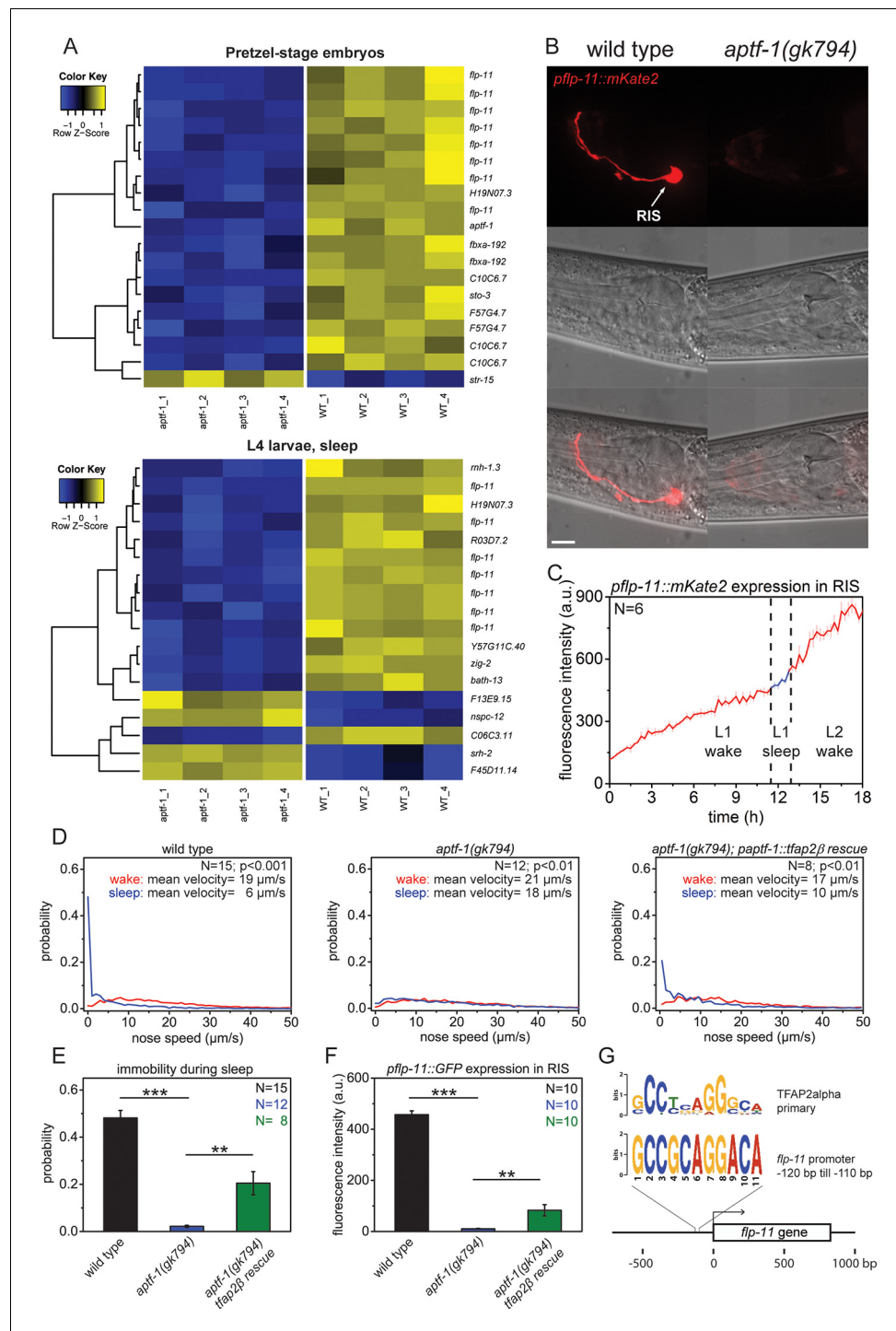


Figure 2. The AP2 transcription factor APTF-1 controls FLP-11 expression in RIS. (A) Transcriptional analysis of *aptf-1(gk794)* mutants revealed genes that are regulated by APTF-1. Wild-type and *aptf-1(gk794)* pretzel-stage embryos and sleeping L4 larvae were used for a transcriptome analysis. In both life stages, expression of the FMRFamide-like neuropeptide FLP-11 was strongly reduced in *aptf-1(gk794)*. This suggests transcriptional control of FLP-11 by APTF-1. Data can be found in **Supplementary file 1**, Tables 1A and 1B. (B) Expression of *pflp-11::mKate2* in wild type and *aptf-1(gk794)*. Expression of mKate2 was absent in RIS in *aptf-1(gk794)* showing that APTF-1 controls expression of FLP-11. Expression of *flp-11* in RIS was reminiscent to the expression of the *flp-11* homolog *afp-6* in RIS in *Ascaris nematodes* (Yew et al., 2007). Expression for additional genes can be found in **Figure 2—figure supplements 2** and **3**. (C) *flp-11* expression profile in RIS over the sleep-wake cycle. Expression

Figure 2 continued on next page

Figure 2 continued

does not change with the sleep-wake cycle. (D) Probability distribution of nose speeds during wake and sleep for wild type, *aptf-1(gk794)* and *aptf-1(gk794); paptf-1::tfap2β* rescue. (E) Comparison of immobility during sleep for wild type, *aptf-1(gk794)*, and *aptf-1(gk794); paptf-1::tfap2β*. The mouse TFAP2β partially rescued the *aptf-1(gk794)* sleep phenotype. (F) Comparison of *pflp-11::GFP* fluorescence intensity in RIS for wild type, *aptf-1(gk794)*, and *aptf-1(gk794); paptf-1::tfap2β*. The mouse TFAP2β partially rescued the expression of *flp-11* in RIS (18% of wild-type level). (G) Analysis of putative AP2-binding sites in the *flp-11* promoter region. The *flp-11* promoter region was scanned for the primary mouse AP2α-binding site. Overlap was found ($p < 0.001$, $q = 0.06$ (Grant et al., 2011)) for one binding site. Statistical test used was Wilcoxon Signed Paired Ranks test. ** denotes statistical significance with $p < 0.01$, *** denotes statistical significance with $p < 0.001$. Scale bar is 10 μm .

DOI: [10.7554/eLife.12499.005](https://doi.org/10.7554/eLife.12499.005)

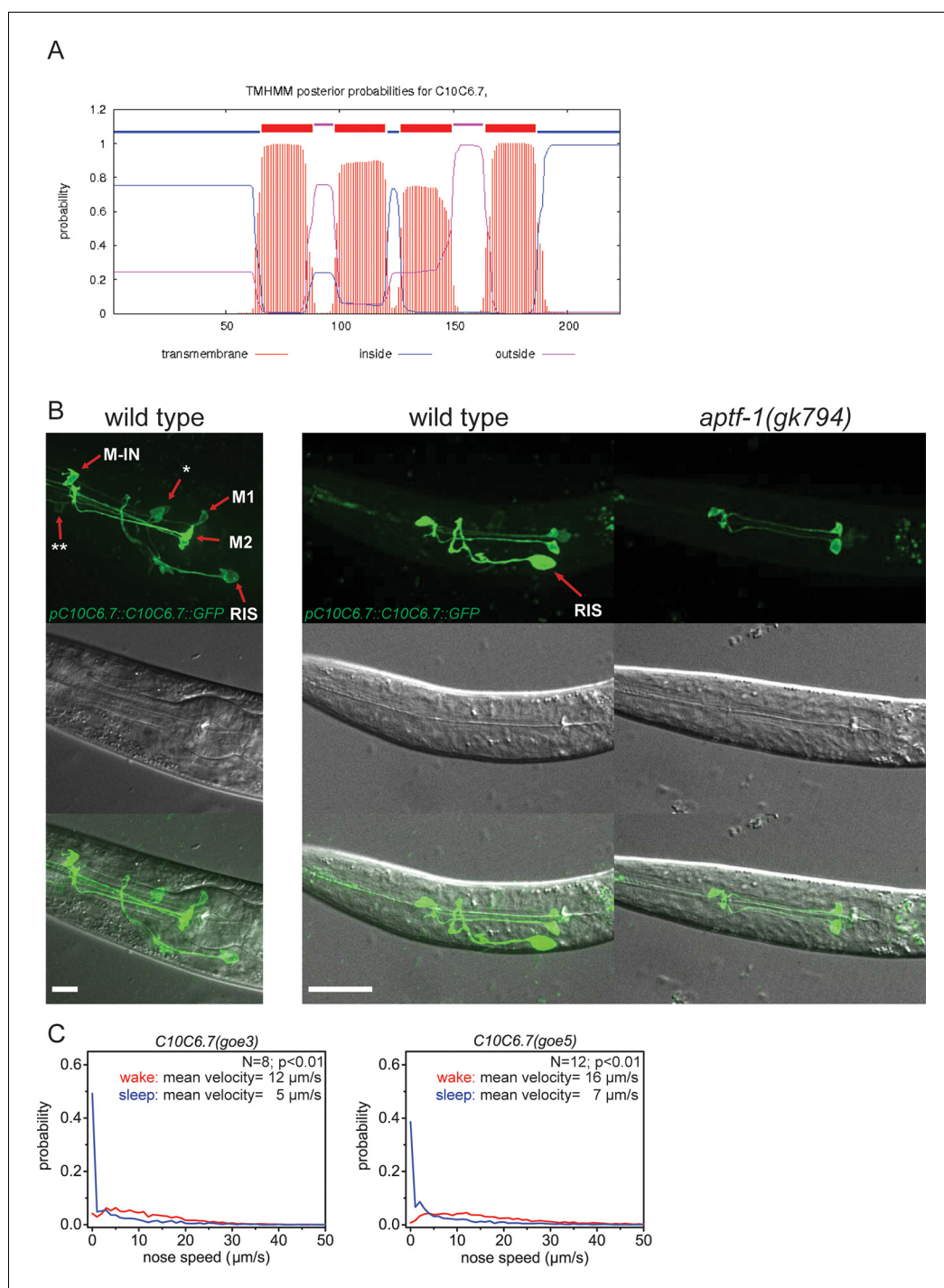


Figure 2—figure supplement 1. C10C6.7 is a putative four transmembrane helix protein that is expressed in RIS and that is controlled by *aptf-1*. (A) Bioinformatics analysis suggests that C10C6.7 is a four transmembrane helix protein (Krogh et al., 2001). (B) Expression pattern of GFP-tagged fosmids for C10C6.7. Expression is visible in nine cells: interneuron RIS; pharyngeal neurons M1, M2, Motor-interneuron (M-IN), an unidentified pair of pharyngeal neurons (**), and an unidentified pair of sensory neurons (*). Expression of C10C6.7 protein in RIS is controlled by *aptf-1*. (C) Probability distribution of nose speeds during wake and sleep for *C10C6.7(goe3)* and *C10C6.7(goe5)* shows that C10C6.7 does not play a significant role in sleep control. Statistical test used was Wilcoxon Signed Paired Ranks test. Scale bars are 10 μm .

DOI: 10.7554/eLife.12499.006

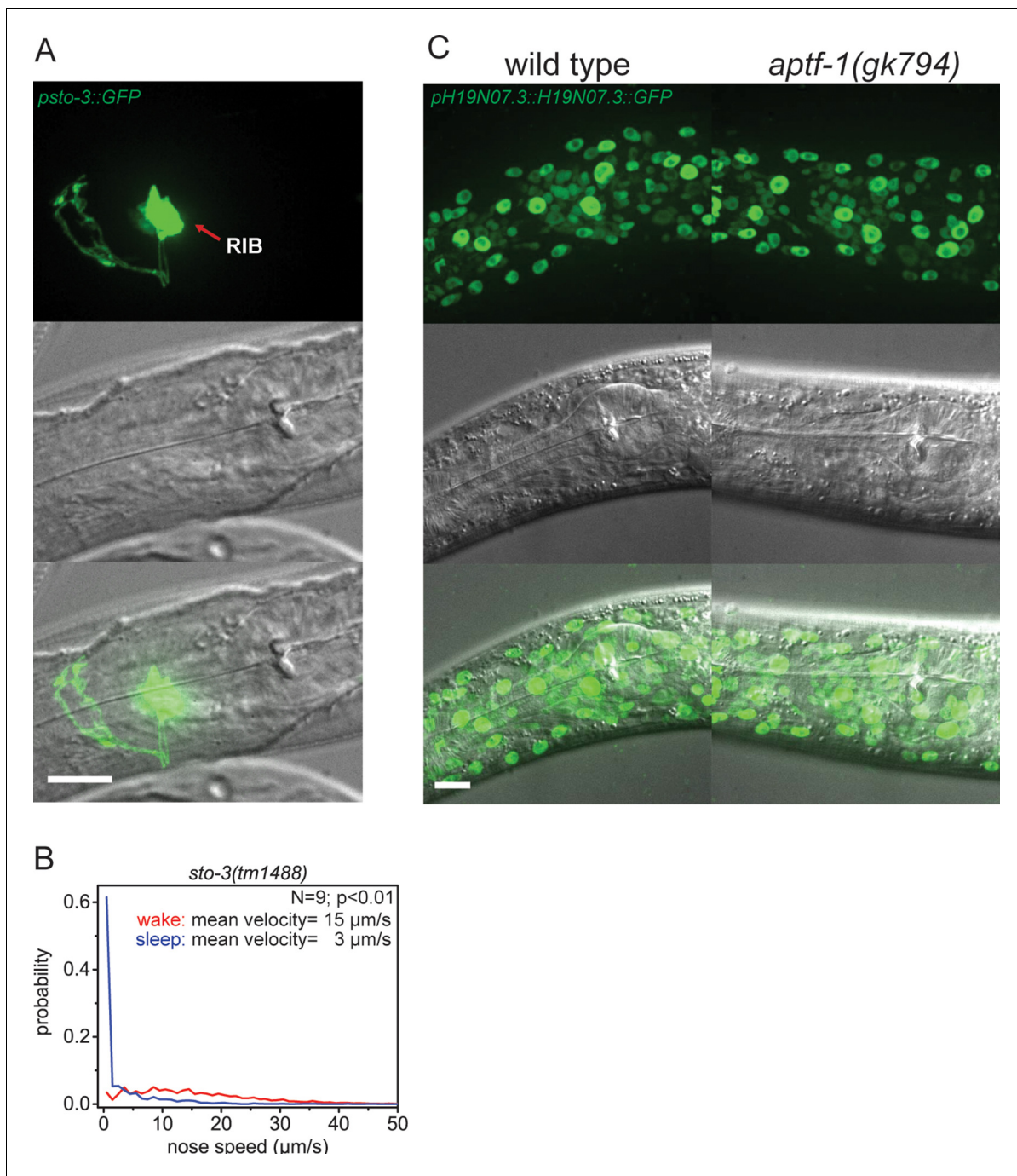


Figure 2—figure supplement 2. Expression pattern of *sto-3* and *H19N07.3*. (A) Expression pattern of *sto-3* promoter fusions. *STO-3* is expressed in RIB neuron and additionally in three unidentified non-neuronal cells in the tale (not shown). (B) Probability distribution of nose speeds during wake and sleep for *sto-3(tm1488)* shows that *sto-3* does not play a significant role in sleep control. (C) Expression pattern of GFP-tagged fosmids for *H19N07.3*. The *H19N07.3* protein is expressed in all somatic cell nuclei, but its levels are not regulated by *aptf-1*. Statistical test used was Wilcoxon Signed Paired Ranks test. Scale bars are 10 μm .

DOI: 10.7554/eLife.12499.007

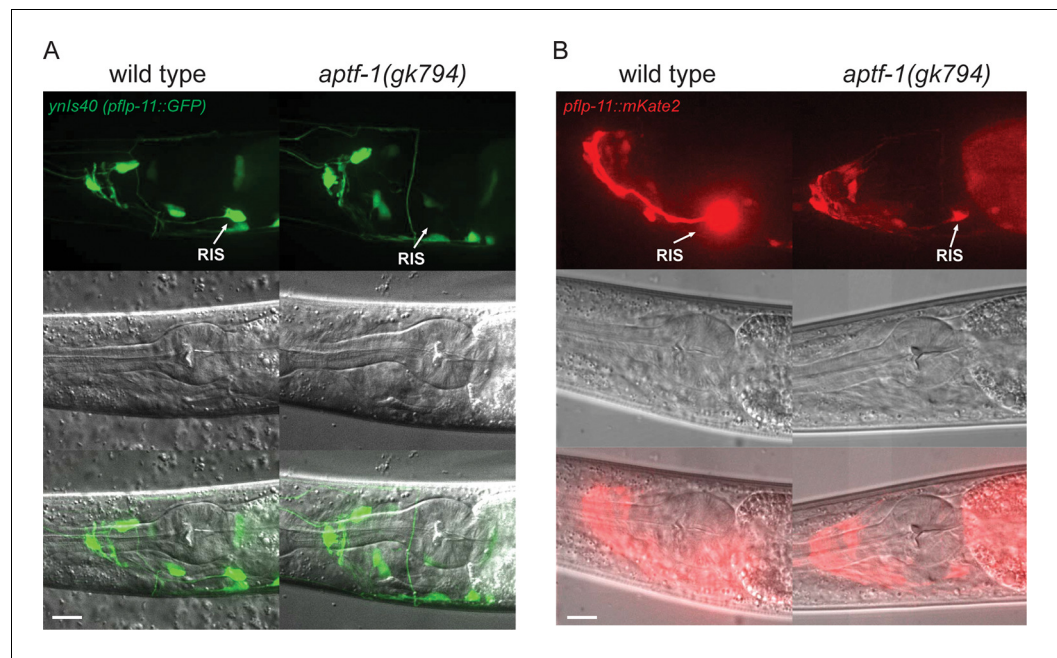


Figure 2—figure supplement 3. FLP-11 is strongly expressed in RIS and weakly in additional neurons. APTF-1 controls the expression in RIS. (A) Expression pattern of *ynls40(pflp-11::GFP)* in wild type and *aptf-1(gk794)* mutant. The transgene expresses in several neurons including RIS. *aptf-1(gk794)* abolishes the expression specifically in RIS. (B) Expression pattern of *goels288(pflp-11::mKate2)* in wild type and the *aptf-1(gk794)* mutant. Strong expression is visible only in RIS. By increasing the contrast to the point where RIS is over-saturated several additional neurons becomes visible that may be identical to those seen in *ynls40* (Kim and Li, 2004). *aptf-1(gk794)* strongly reduces the expression specifically in RIS. Scale bars are 10 μ m.

DOI: [10.7554/eLife.12499.008](https://doi.org/10.7554/eLife.12499.008)

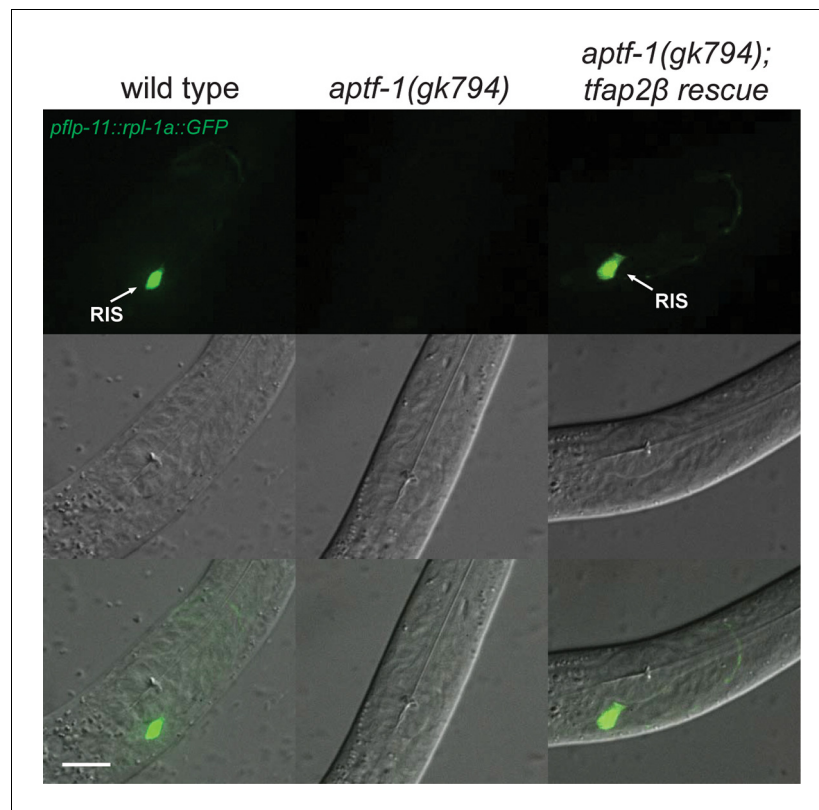


Figure 2—figure supplement 4. Mouse TFAP2beta partially restores expression of *flp-11* neuropeptides in RIS in *aptf-1* mutant worms. Expression of *pflp-11::GFP* in wild type, *aptf-1(gk794)*, and *aptf-1(gk794); tfap2beta rescue*. In *aptf-1(gk794)*, expression of *flp-11* is strongly reduced but could partially be restored by the mouse TFAP2beta. Expression of *flp-11::GFP* in the rescue strain varied between 5–50% of wild-type levels. Here, we show a picture of 50% rescue. Scale bar is 10 μ m.

DOI: [10.7554/eLife.12499.009](https://doi.org/10.7554/eLife.12499.009)

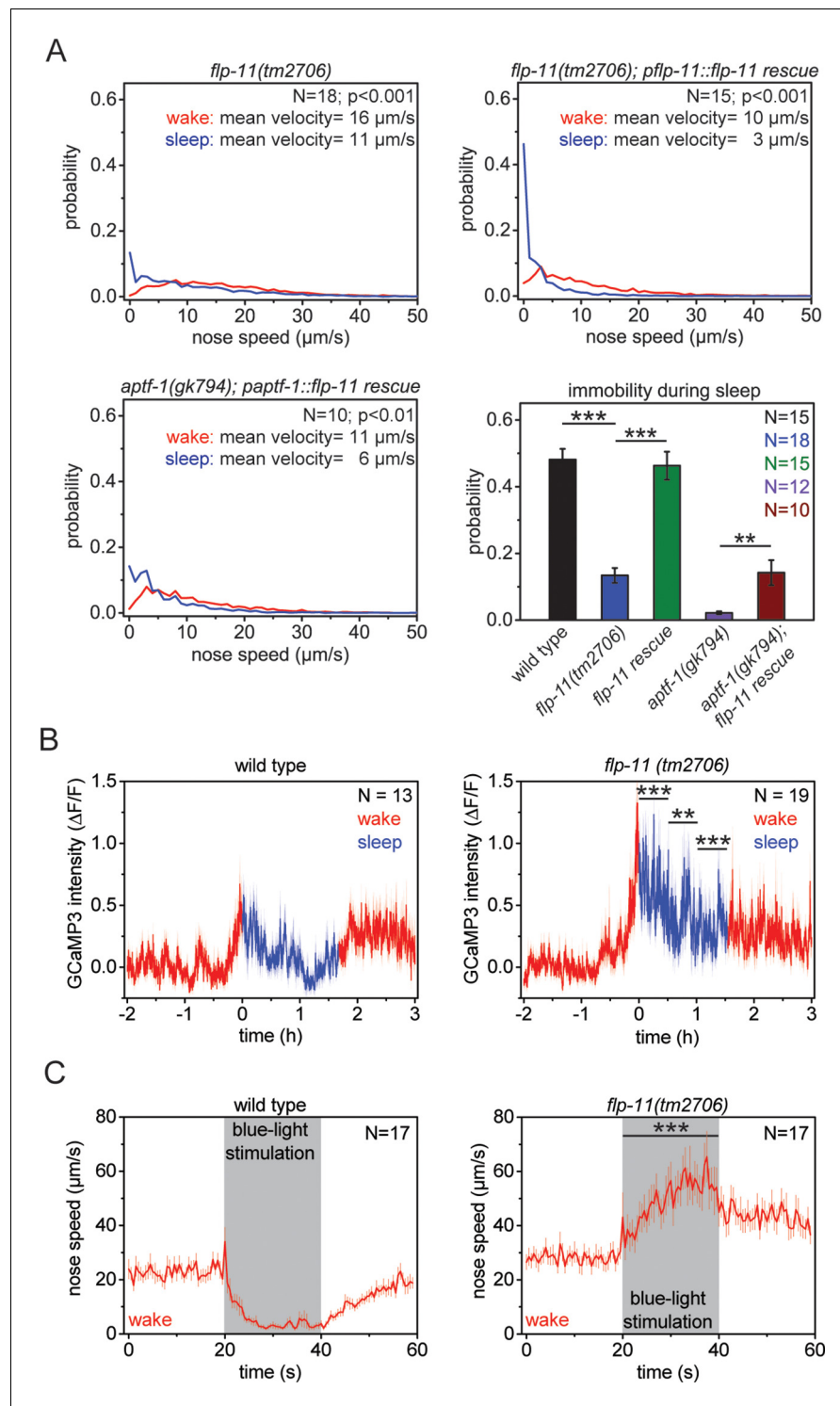


Figure 3. RIS induces sleep through the sleep-inducing FMRFamide-like neuropeptide FLP-11. **(A)** Probability distribution of nose speeds during wake and sleep for wild type, *flp-11(tm2706)*, *flp-11(tm2706); pflp-11::flp-11* rescue and *aptf-1(gk794); paptf-1::flp-11* rescue. Immobility during the time the animal should be sleeping was substantially reduced in *flp-11(tm2706)*. *flp-11(tm2706)* could be rescued by expression of the wild-type *flp-11* gene. Furthermore, expression of *flp-11* in *aptf-1(gk794)* partially rescued sleep behavior. **(B)** Averaged RIS calcium activity pattern across time in wild type and *flp-11(tm2706)*. RIS was strongly activated at the onset of sleep in *flp-11(tm2706)* (Student's t-test). **(C)** Channelrhodopsin-2 activation of *aptf-1*-expressing neurons caused immediate immobility in wild type. In contrast, *flp-11(tm2706)* accelerated upon blue light stimulation showing that RIS-
Figure 3 continued on next page

Figure 3 continued

dependent immobility is impaired. Statistical tests used were Wilcoxon Signed Paired Ranks test for comparisons within genotypes and Student's t-test for comparisons between genotypes. Error bars are SEM. ** denotes statistical significance with $p < 0.01$, *** denotes statistical significance with $p < 0.001$.

DOI: [10.7554/eLife.12499.010](https://doi.org/10.7554/eLife.12499.010)

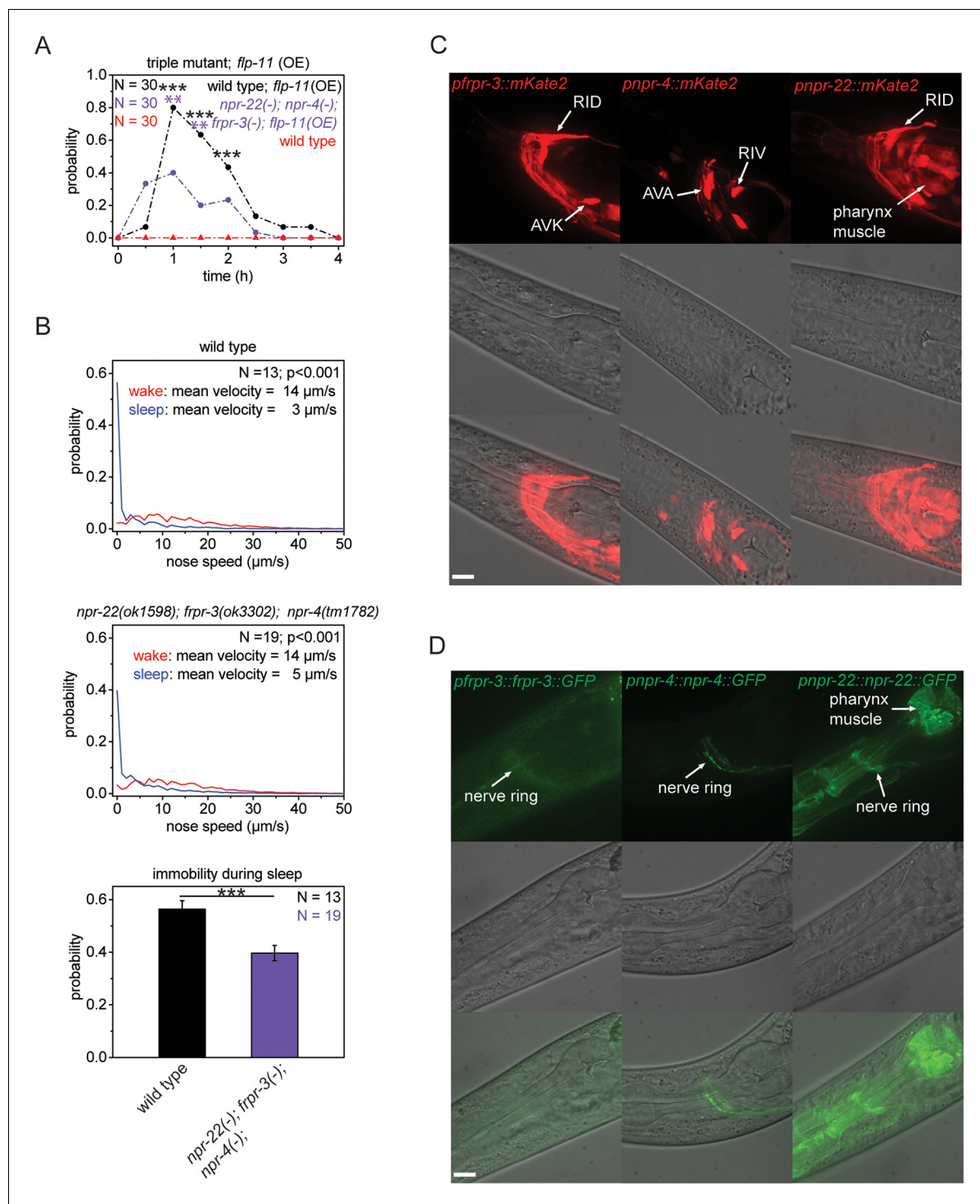


Figure 4. Multiple receptors may be involved in sleep induction. (A) Behavioral analysis over time after the heat-shock-induced overexpression of *flp-11* in wild-type and the *npr-22(ok1598); frpr-3(ok3302); npr-4(tm1782)* triple mutant. To assess the effect of the heat shock on quiescence, wild-type worms without *flp-11* overexpression were analyzed at the same time and do not show any behavioral changes. Overexpression of *flp-11* caused anachronistic quiescence that was lasting approximately 1 hr in the wild type. Quiescence was significantly reduced by approximately 50% in the triple mutant. (B) Probability distribution of nose speeds during wake and sleep for wild type and *npr-22(ok1598); frpr-3(ok3302); npr-4(tm1782)* triple mutant. Immobility during sleep was reduced by about 30% in the *npr-22(ok1598); frpr-3(ok3302); npr-4(tm1782)* triple mutant. (C) Expression patterns of *frpr-3*, *npr-4* and *npr-22* promoter fusions. FRPR-3 is expressed in about 30 neurons, mostly in the head. Expression of NPR-4 was seen in about five neurons. NPR-22 was expressed in several neurons and muscle tissue including pharynx and head muscle. (D) Expression patterns of GFP-tagged fosmids for *frpr-3*, *npr-4*,
 Figure 4 continued on next page

Figure 4 continued

and *npr-22*. FRPR-3 and NPR-4 were mostly expressed around the nerve ring. NPR-22 localized broadly to the plasma membrane in several neurons, pharynx muscle, head muscle, and the anal sphincter muscle. Statistical tests used were Wilcoxon Signed Paired Ranks test for comparisons within genotypes and Student's t-test for comparisons between genotypes. Error bars are SEM. ** denotes statistical significance with $p < 0.01$, *** denotes statistical significance with $p < 0.001$. Scale bars are 10 μm .

DOI: [10.7554/eLife.12499.011](https://doi.org/10.7554/eLife.12499.011)

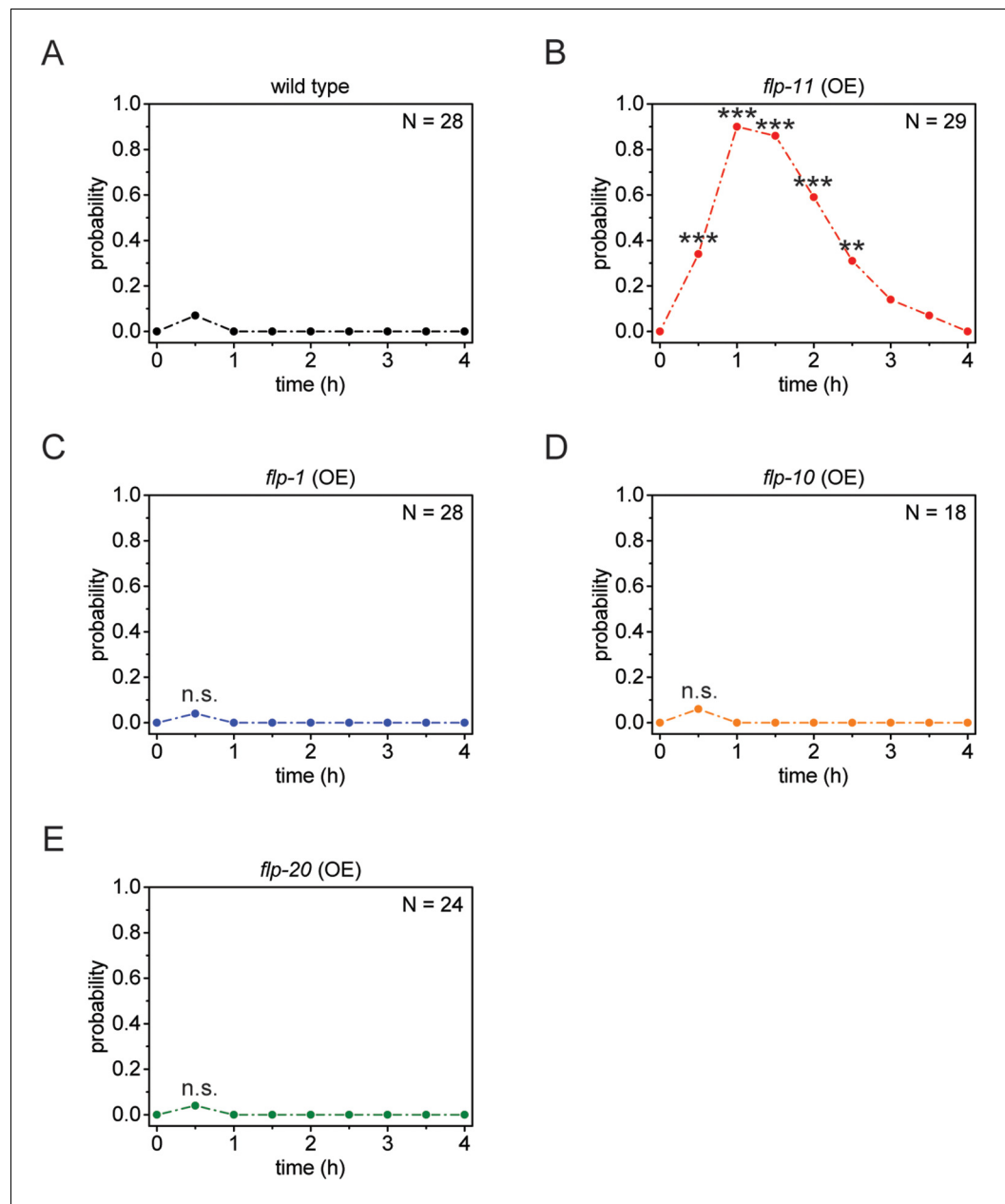


Figure 4—figure supplement 1. Heat-shock-induced *flp-11* overexpression causes quiescence but heat-shock-induced overexpression of three other *flp* genes does not, suggesting that quiescence cannot be induced by overexpression of any *flp*. (A) Behavioral analysis of wild-type adult worms over time after 5 min of heat shock at 37°C. (B–E) Behavioral analysis of wild-type adult worms over time after heat shock-induced overexpression of *flp-11*, *flp-1*, *flp-10*, and *flp-20*. Only heat-shock-induced overexpression of *flp-11* induces quiescence.

DOI: [10.7554/eLife.12499.012](https://doi.org/10.7554/eLife.12499.012)

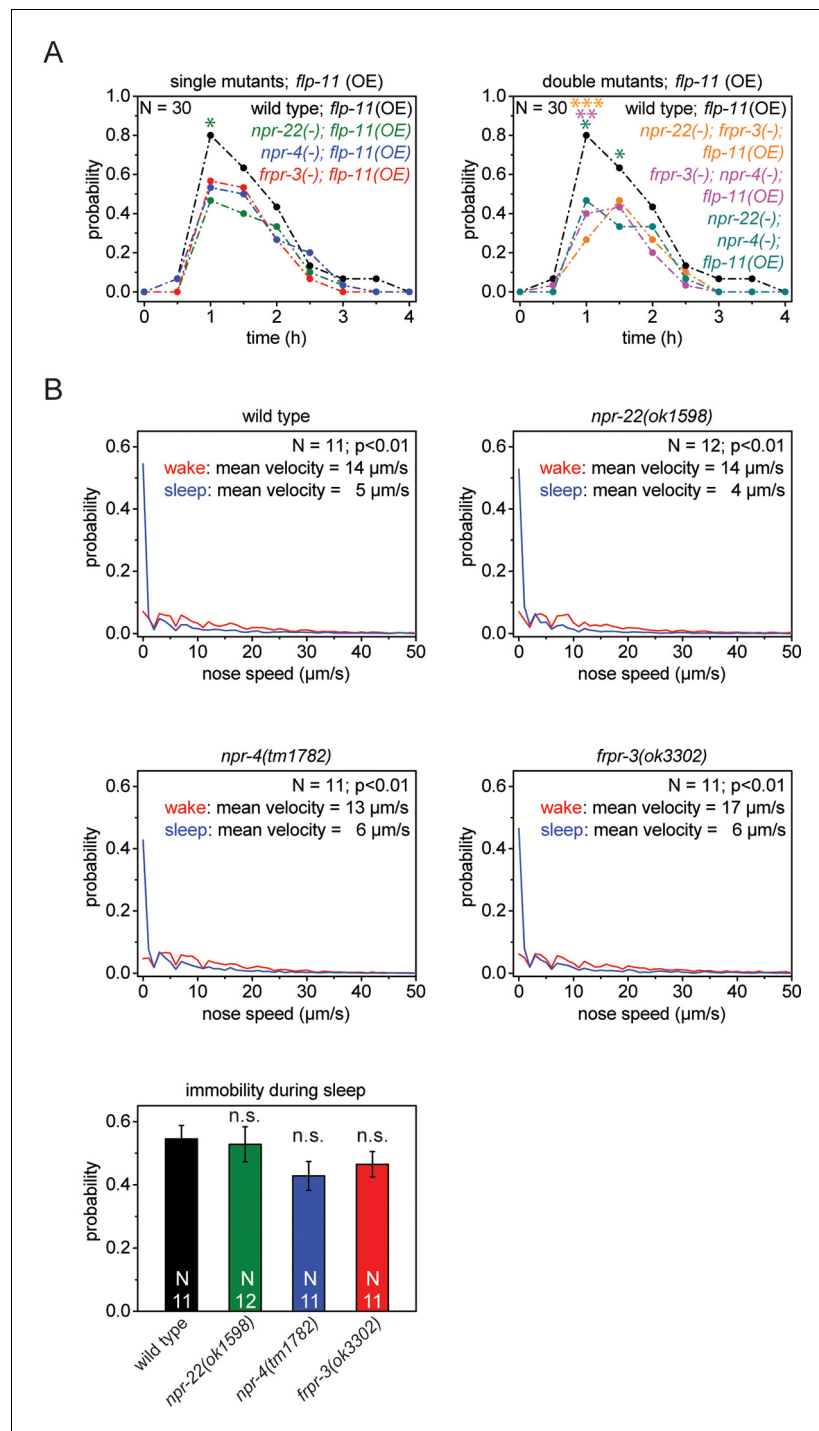


Figure 4—figure supplement 2. Single receptors mutants do not show reduced quiescence during sleep, but do show reduced quiescence upon heat-shock-induced overexpression of *flp-11*. (A) Heat shock-induced overexpression of *flp-11* in single and double mutants of *frpr-3(ok3302)*, *npr-4(tm1782)*, and *npr-22(ok1598)*. The strength of the anachronistic quiescence correlates with the combination of receptors ranging from highest for single mutants to lowest for the double mutants. (B) Probability distribution of nose speeds during wake and sleep for wild type and *npr-22(ok1598)*, *frpr-3(ok3302)*, *npr-4(tm1782)* single mutants. Immobility during sleep is not significantly different between wild type and single mutants. Statistical tests used were Wilcoxon Signed Paired Ranks test for comparisons within genotypes and Student's t-test for comparisons between genotypes. Error bars are SEM. *denotes statistical significance with $p < 0.05$, **denotes statistical significance with $p < 0.01$, *** denotes statistical significance with $p < 0.001$.

Figure 4—figure supplement 2 continued on next page

Figure 4—figure supplement 2 continued

DOI: [10.7554/eLife.12499.013](https://doi.org/10.7554/eLife.12499.013)

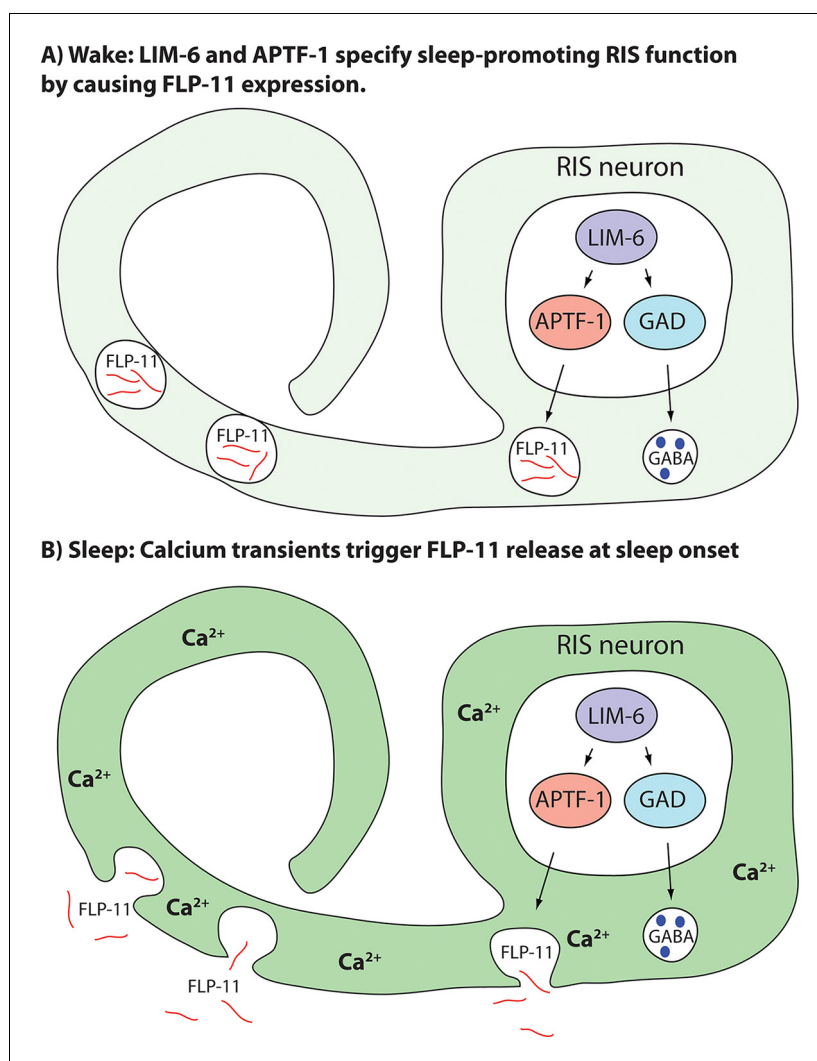


Figure 5. Model for generation of sleep-promoting function of RIS and sleep induction by RIS. According to this model, the transcription factor LIM-6 controls GABAergic and peptidergic function in RIS in parallel. To render this neuron sleep-promoting, LIM-6 is required for the expression of the APTF-1 transcription factor. APTF-1, in turn, is required for the expression of sleep-inducing FLP-11 peptides. FLP-11 is present in RIS at all times. Sleep onset is triggered by an unknown signal, which leads to a depolarization and to calcium influx. This triggers FLP-11 release, which in turn systemically induces sleep behavior.

DOI: [10.7554/eLife.12499.014](https://doi.org/10.7554/eLife.12499.014)